Revised version submitted to the Journal of Applied Physics

Enhancing CO_2 plasma conversion using metal grid catalysts

E. J. Devid*,[1,2,a,b)], M. Ronda-Lloret*,[3)], D. Zhang[4)], E. Schuler[3)], D. Wang[1)], C.-H. Liang[1)], Q. Huang[1,5)], G. Rothenberg[3)], N. R. Shiju[3)], A. W. Kleyn[1b)]

AFFILIATIONS

1) Center of Interface Dynamics for Sustainability, Institute of Materials, China Academy of Engineering Physics, 596 Yinhe Road 7th section, Chengdu, Sichuan 610200, People's Republic of China

2) DIFFER - Dutch Institute for Fundamental Energy Research, De Zaale 20, 5612AJ, Eindhoven, The Netherlands

3) Van 't Hoff Institute for Molecular Sciences, Faculty of Science, University of Amsterdam, P.O. Box 94157, 1090GD, Amsterdam, The Netherlands

4) Leiden Institute of Chemistry, Leiden University, Einsteinweg 55, 2333CC, Leiden, The Netherlands

5) School of Optoelectronic Engineering, Chongqing University of Posts and Telecommunications, Chongqing 400065, People's Republic of China

[a)] **Electronic mail:** ejdevid@outlook.com

[b)] **Authors to whom correspondence should be addressed:** ejdevid@outlook.com; a.w.kleijn@contact.uva.nl

*: **these authors contributed equally to this paper.**

ABSTRACT

The synergy between catalysis and plasma chemistry often enhances the yield of chemical reactions in plasma-driven reactors. In the case of CO_2 splitting into CO and O_2, no positive synergistic effect was observed in earlier studies with plasma reactors, except for dielectric barrier discharges, that do not have high yield and high efficiency. Here we demonstrate that introducing metal meshes into a radio-frequency driven plasma reactors increases the relative reaction yield by 20 to 50%, while supported metal oxide catalysts in the same setups have no effect. We attribute this to the double role of the metal mesh, which acts both as catalyst for direct CO_2 dissociation as well as for oxygen recombination.

I. INTRODUCTION

Using CO_2 as a renewable carbon feedstock for making chemicals and fuels is essential in the mitigation of climate change,[1] and with it for meeting the goals of the Paris Agreement.[2] Converting CO_2 into solar fuels is an important step along this pathway[1]. There are several ways of doing this, including thermal catalysis, electrochemical conversion and plasma conversion. [3-5] The last option is

especially attractive, as plasma reactors have the promise to exclusively excite the CO_2 molecules vibrationally, thus reducing the overall thermodynamic penalty incurred when using CO_2 as a reactant. Several studies report that CO_2 and/or CH_4 can be converted by plasma into CO and syngas (a mixture of CO and H_2), which can be used as feedstocks by the chemical industry. [4, 6-17] Most of these studies use Dielectric Barrier Discharges (DBD) reactors.[4] However, the conversions and energy efficiencies from DBD reactors, in particular for CO_2 splitting, are low (conversion ~30-45%, efficiency ~5-10%) even in the presence of catalysts.[4] Microwave (MW) and radio frequency (RF) plasma can yield higher conversions and energy efficiencies of up to 50%.[18, 19] For such plasma technologies, little is known about the effects of catalysts. Spencer and Gallimore studied the effect of adding a catalyst to a high-power RF discharge,[20, 21] and found it to be negative**.**

Building on our experiments with plasma-assisted reactions,[22-28] we approached the problem of high-yield CO_2 activation in plasma reactors from another angle. Recent experiments on NH_3 production from N_2 and H_2 using RF plasma show that using a catalyst can increases the ammonia yield. [29] This is due to the introduction of different type of metal meshes in the RF reactor.[29] The authors attribute the catalytic effect to the formation of a thin metal film on the reactor wall. The catalytic action mainly takes place on the film. From numerical simulations, the authors concluded that dissociation of N_2 and H_2 is induced by plasma, while the formation of the NH_3 product occurs via a Langmuir-Hinshelwood reaction on the catalyst surface.[29] In other studies on ammonia synthesis by plasma, catalysis also significantly increases the product yield. The increased yield was attributed to catalysis on surfaces. Several reactors types were used in these studies.[30-37] Encouraged by the results reported for ammonia synthesis, we studied the effects of metal meshes on CO_2 conversion in RF plasma reactors. We found that introducing a pure metallic mesh considerably enhances CO_2 dissociation. The present work has a very strong focus to study the increase by catalysis of the CO_2 conversion in a RF plasma reactor.

CO_2 dissociation at surfaces was studied under low pressure and surface science conditions using ultra high vacuum (UHV).[38, 39] Dissociative adsorption of thermal CO_2 on low index faces of Cu or Ni single crystals is unlikely (1% level or below). Translational activation of CO_2 increases its probability to dissociate to 10%. However, in a non-thermal plasma, translational activation is unlikely because the neutral gas is close to room temperature. It was found that on stepped Cu surfaces dissociation of CO_2 does occur in UHV.[40, 41] In fact, CO_2 dissociation does occur on a variety of stepped metal surfaces (but not on metal oxides).[42, 43] Dissociation and dissociative adsorption may be promoted by vibrational excitation. Modelling of CO_2 plasma using DFT calculations of dissociative adsorption of CO_2 on Ni demonstrates that vibrational excitation assists dissociation into CO and adsorbed oxygen atoms (O_{ads}). [44, 45] A recent theoretical study indicates that surface-induced dissociation can be enhanced by adding a strong electric field of typically 10 V/nm.[46] Such field strengths are possible in electrochemistry, but not in a plasma reactor.

The interaction of atomic oxygen with metal surfaces was studied extensively. Several phases of surface oxides are formed on Cu(100) and Cu(110) before bulk oxidation, see e.g. [47-49]. For Ag and other metal surfaces, Killelea and co-workers recently reported detailed studies in which the surfaces are exposed to atomic oxygen directly.[50-54] A number of surface geometries or phases depending on the conditions is again observed in Scanning Tunneling Microscopy. This work demonstrates that the interaction of atomic oxygen, that is present in plasma reactors, can initiate a complex set of reactions on pure metal surfaces. Exposing metals to atomic oxygen leads to a self-limiting growth of a surface oxide. There is no oxidation of the bulk after formation of a thick surface oxide.[55, 56] There are no studies in the literature to our knowledge in which metal oxides are directly exposed to atomic oxygen.

Besides the classical catalytic dissociation of CO_2 in a Langmuir-Hinshelwood mechanism, surface collisions can also induce dissociation, as proven by Yao et al. [57] They showed that dissociation of CO_2^+ ions on surfaces can occur upon impact, when the translational energy of the ions is around 20 eV or higher. However, non-thermal RF plasmas contain very few positive ions, so this process is unlikely to yield large amounts of CO.

Here we study the role of catalysts in CO_2 splitting driven by RF plasma. We find that the introduction of purely metallic meshes enhances the dissociation of CO_2, therefore acting as catalysts. XPS and SEM analysis demonstrates that there is no uptake of oxygen by the metal. We propose that the metal enhances the re-combinative desorption of O-atoms to yield O_2. In addition, metallic meshes enhance the dissociation of vibrationally excited CO_2, while metal oxides supported on inert materials are inactive under the same conditions.

II. EXPERIMENTAL CONFIGURATION

A. Reactors

Two sets of experiments were carried out in cylindrical RF plasma reactors described earlier.[23, 25, 28] Details of the wide tube plasma reactor configuration are given in the Supplementary Material (see also Fig. S1). Briefly, the plasma is confined by a quartz tube, surrounded by a 6-turn coil producing a Radio Frequency Inductively Coupled Plasma (RF-ICP). The composition of the exhaust gas produced in the reactor is measured on-line, in real time by a quadrupole mass spectrometer (QMS). No attempt was made to optimize the energy efficiency of the reactor as the purpose of this work is to study catalytic effects on the CO_2 splitting process.

Two versions of plasma reactor setups were used. The differences between the wide tube plasma reactor versus the narrow tube plasma reactor are mainly in the actual size of the reactor tubes and the mounting geometry of the catalyst. Both setups are described in detail in the Supplementary Material (Fig. S1–S6).

B. Catalyst preparation, thermal reactions and characterization

The supported catalysts were prepared by wet impregnation as described in the Supplementary Material. These oxide catalysts were introduced into the plasma reactor by two different methods, as described in the Supplementary Material.

A different type of catalytic material was also tested. It consists of commercially available purely metallic mesh that also can be seen as foam based meshes with high transparency. This Cu mesh is put either in the inner tube in the plasma region between the windings of the RF coil or downstream behind the coil.

The thermal catalytic tests were carried out under atmospheric pressure in an automated six-flow parallel reactor system. It consists of six individual fixed-bed quartz reactors located in a furnace.[58] The reactants and products were analyzed with a gas chromatograph (Interscience microGC, with FID and TCD detectors).

The supported catalyst pellets inserted in the catalyst holder were in situ reduced via Ar-H_2 plasma (i.e. 20% H_2 : 80% Ar plasma with total flow of 250 sccm). The Ar-H_2 plasma for the reduction of the

catalyst pellets lasted 1 hour where the input power was constant at 300 W. The pressure in the narrow tube plasma reactor was 100 Pa.

Details on the characterization techniques of the catalysts, the catalyst holder and the metal mesh capsule is presented in the Supplementary Material.

III. RESULTS AND DISCUSSION

Results obtained with the wide tube plasma reactor are shown in Fig. 1. Plotted is the CO_2 conversion towards CO, defined by $I(CO_{out})/ I(CO_{2,\,in})$. Here $I(CO_{out})$ is the corrected CO QMS intensity measured at the exhaust of the reactor and $I(CO_{2,\,in})$ is the CO_2 intensity measured with the plasma off, i.e. the incident CO_2 flow. It should be noted that the conversion into other products such as carbon or C_2 was not observed and is very low. The CO_2 conversion is plotted as a function of the specific energy input: the RF power per molecule in the flow. This quantity is varied by varying the RF power or the CO_2 flow. Experimental conditions are given in the figure caption. It should be noted that in case of a changing CO_2 flow the CO_2 conversion scales with the specific energy input.[25] This is apparent from the fact that the results for an empty reactor are the same for flows of 100 and 200 sccm CO_2. Therefore, the results with metal meshes can be directly compared to results for supported catalysts measured at the same specific energy. When plasma alone was done (i.e. a CO_2 plasma in an empty plasma reactor without catalyst), the CO_2 conversion was around 30% at a specific energy input of 20 eV. The conversion was higher when placing the copper mesh downstream in the plasma region. Remarkably, an even higher CO_2 conversion was obtained when the Cu mesh was placed directly within the plasma field (see the green triangles curve in Fig. 1). At a specific energy input of 20 eV, the CO_2 conversion reached 50%, showing a synergistic effect of plasma and metal mesh in enhancing CO_2 splitting.

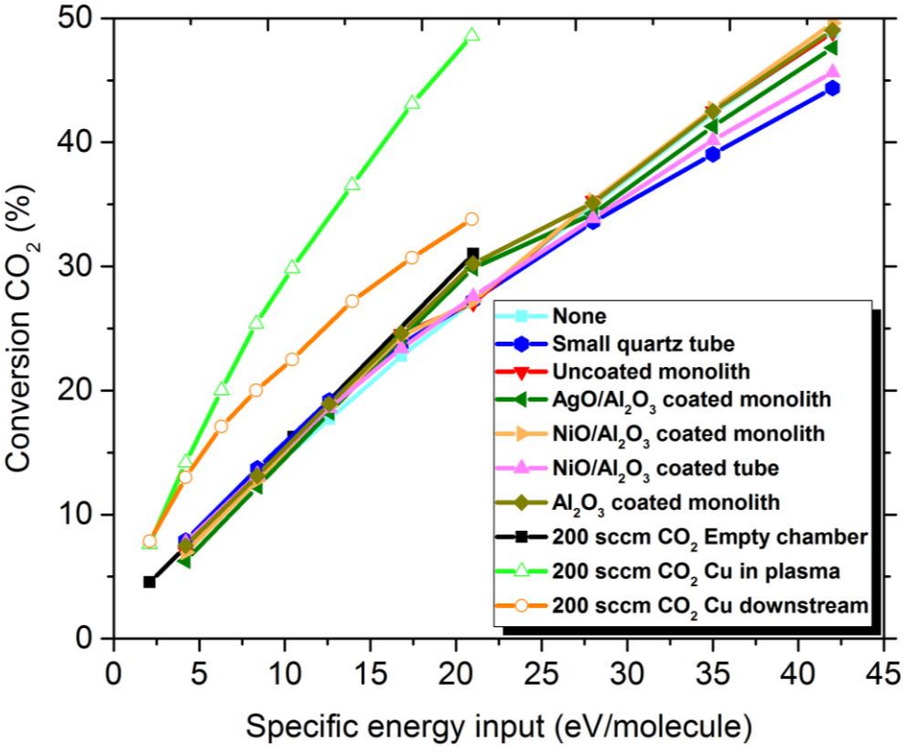

FIG 1. CO_2 conversion in the wide tube plasma reactor as a function of the specific energy input. The RF power is varied between 0 and 300 W. For oxide supported catalysts the CO_2 flow is 100 sccm (Standard Cubic Centimeters per Minute), and the pressure is about 100 Pa. In the case of the metallic Cu mesh inserted in the plasma reactor, the flow is 200 sccm and all other conditions are similar compared to the oxide supported catalyst testing. "Cu in the plasma" refers to that the Cu mesh is placed between the windings of the coil in the wide tube plasma reactor. Similarly, "Cu downstream" refers to that the Cu mesh is placed after the coil and before the flow exit of the wide tube plasma reactor.

A. Supported oxidic catalysts

We now focus on the conversion obtained with supported oxide catalysts. In Fig. 1, we can see that when using AgO/Al_2O_3 coated monolith, NiO/ Al_2O_3 coated monolith, NiO/ Al_2O_3 coated tube and Al_2O_3 coated monolith in the wide tube plasma reactor the CO_2 conversion doesn't increase significantly compared to the plasma alone reference with no presence of catalyst. For other combinations of metal in the oxide and support materials also no significant reactivity is seen. One possible explanation is that most molecules in the flow do not interact sufficiently with the catalyst surface, especially in the case of the coated inner tube structure, see Fig. S2. To check if the way of introducing the catalyst in the plasma reactor is relevant, we carried out experiments with the narrow tube plasma reactor. Here the plasma flow percolates through the catalyst bed inside the catalyst holder, held in place between two Cu meshes perpendicular to the plasma flow. In this way the catalyst is in close contact with the plasma flow. The results are shown in Fig. 2.

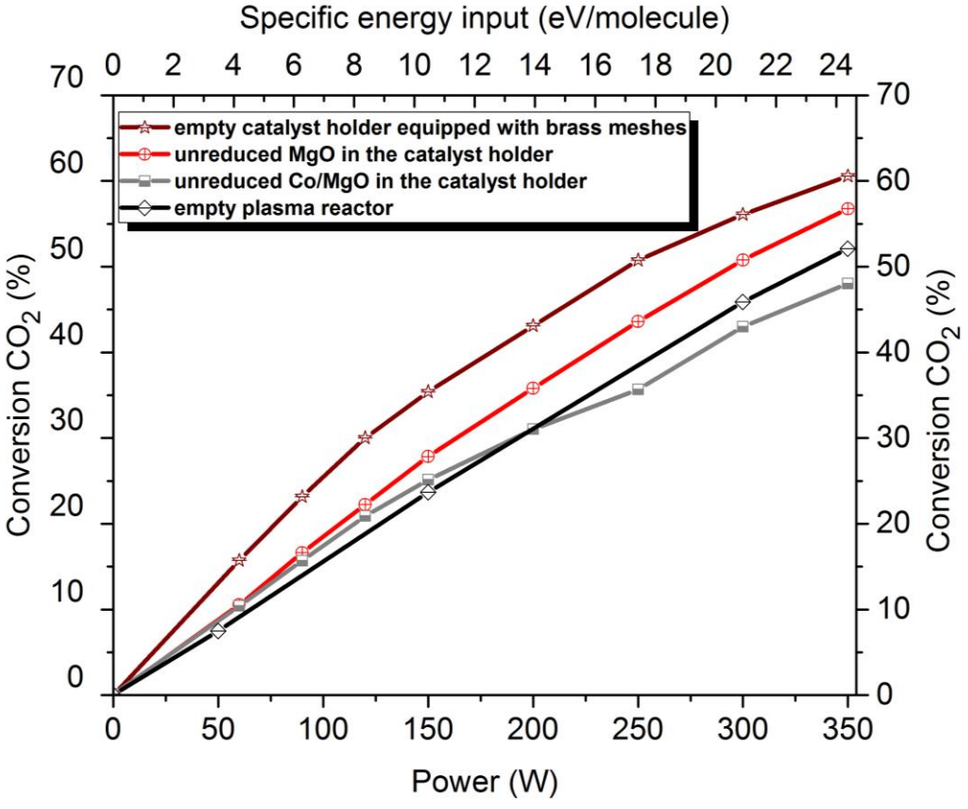

FIG. 2. CO_2 conversion in the narrow tube plasma reactor as a function of the specific energy input and the RF power. The RF power is varied between 0 and 350 W. The CO_2 flow is 200 sccm, the pressure is about 100 Pa. The black curve represents CO_2 splitting where its performance without the use of a catalyst holder and its metal grids is measured. The brown stars curve in Fig. 2 is measured for an empty catalyst holder, but with the metal Cu grids in place. The red crossed circled curve is measured with a catalyst holder filled with pure MgO pellets, and the grey curve represents data for a MgO supported Co_3O_4 catalyst.

Fig. 2 shows that adding Cu meshes to the empty narrow tube plasma reactor increases the CO_2 conversion by a factor of about 1.2. Adding MgO pellets in the catalyst compartment of the catalyst holder between the Cu grids decreases the CO yield with respect to the empty metallic cell within the catalyst holder but increases the CO yield with respect to the empty narrow tube plasma reactor. This indicates that MgO is slightly catalytically active. Adding the 5wt.% Co_3O_4/MgO supported catalyst only decreases the CO_2 conversion with respect to CO_2 plasma at the MgO catalyst in the narrow tube plasma reactor. This might be due to deactivation of active sites on the clean MgO catalyst by adsorbed Co. Other Co/MgO supported metal oxide catalysts with higher metal content show similar results. From the data in Fig. 1 and Fig. 2, we conclude that **adding a supported metal oxide catalyst does not enhance the CO yield by RF-ICP**. The experiments with the narrow tube plasma reactor show that the lack of enhancement cannot be due to limited interaction between catalyst and CO_2 plasma flow.

In this set of experiments, we determined the temperature of the metal grids using a pyrometer. The highest temperature observed was 420 °C, at a power level of 350 W. Such temperatures are

sufficient to remove hydrocarbon contamination from the surfaces, but are far too low to induce thermal decomposition of CO_2.[4, 19]

Operating the RF-ICP at 1000 Pa does not introduce significant changes in the CO_2.conversion. Therefore, lack of enhancement regarding the conversion of CO_2 for oxide catalysts cannot be explained by the low operation pressures of typically 100 Pa. For a unimolecular dissociation reaction, the low pressure should not be important. In this case the only function of the catalyst is to break an O-CO bond, which is independent of pressure. However, vibrational excitation of the CO_2 may be required to enhance the dissociation. In case of a metallic catalyst, the excited molecules will directly impinge on the metal and dissociate. In case of a supported catalyst the active metal will be inside the metal oxide structure. In this case the excited CO_2 will be quenched by the oxide before it can interact with the active sites inside the catalyst. Another possible reason could be that the metal oxide catalyst has not been properly reduced. We have reduced the metal oxide catalyst by exposure to an Ar-H_2 plasma. This plasma driven reduction contains atomic H, which should be very efficient in reducing the metal oxide. However, no effect of reduction of the catalyst was observed. Therefore, we conclude that supported metal oxide catalysts do not enhance CO_2 dissociation in a RF plasma.

Different from thermal catalysis the total (internal + external) surface area of our supported catalysts is most likely not relevant. We have found from BET measurements that our surface areas for N_2 are typically 200 m^2/gram. Typical pore sizes are below 50 nm. Detailed information is added in the supplementary information (table S1). A plasma cannot penetrate these nm-size pores and vibrationally excited molecules are expected to be quenched very quickly when entering the pore.[59] Without plasma, all these materials are completely inactive. See for instance studies on thermal CO_2 dissociation with different catalysts, but where in all cases temperatures exceeding 600 °C are required to run a CO_2 decomposition reaction.[60-62] So the plasma should not be quenched in a pore before interacting with the catalyst.

B. Metal mesh catalysts

By contrast to the Co_3O_4/MgO supported catalyst, inserting metallic catalysts like Cu meshes into the RF reactor does increase the CO yield. For the experiments with the wide tube plasma reactor the metal meshes of Cu do increase the CO_2 conversion by a factor 1.2 when the metal is behind the RF coil. The increase is higher by a factor of 1.8 when the metal mesh is between the windings of the RF coil as seen in Fig. 1. Similar effects are seen in the narrow tube plasma reactor in Fig. 2. An enhancement of the CO_2 conversion is seen for two metallic grids by a factor 1.2. Conversion close to 60% was obtained at a specific energy of about 24 eV. In conclusion, we observe that metal oxide supported catalysts do not enhance the CO_2 conversion at all, while purely metallic structures significantly enhance the CO yield. The precise amount of the enhancement depends on the morphology of the inserted metal and its position in the reactor. [23, 25, 28] **We tested Cu, brass, Co and Fe and the results are that inserting any of these metals in a CO_2 plasma will enhance the yield of CO.** This is an encouraging observation, and it offers within RF-ICP new opportunities for research in plasma driven CO_2 splitting.

We also used the same metallic mesh catalysts in a thermal reactor.[5] There was no CO_2 conversion detected at all for partial CO_2 pressures of 20000 Pa and temperatures up to 900 °C.

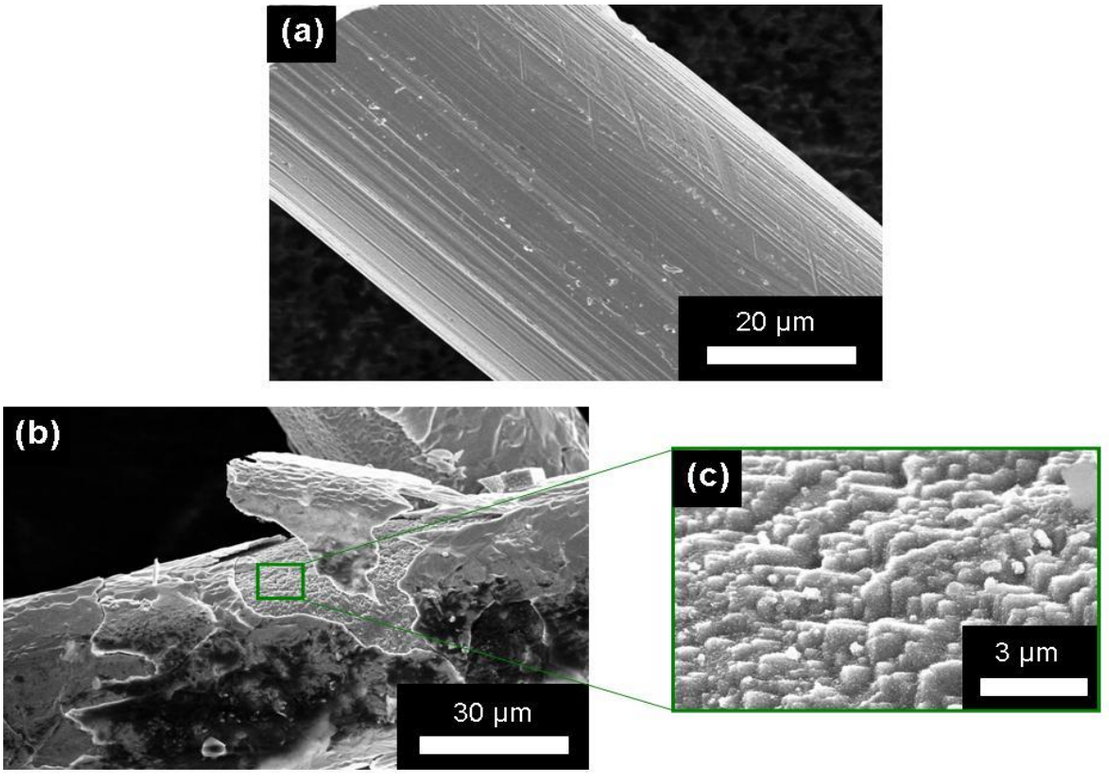

FIG. 3. (a) SEM image of a fresh Cu grid (not exposed to CO_2 plasma). (b) SEM image of a Cu grid exposed to CO_2 plasma. (c) Magnification of Fig. 3b.

To get more insight into the catalytic behaviour of the metal meshes, they were examined by SEM and XPS. The SEM images in Fig. 3 show that surface modification has occurred on the CO_2 plasma exposed Cu grid. Especially Fig. 3c shows the zoomed-in SEM image; after CO_2 plasma exposure the surface of the metal grid has become rough. The roughed Cu oxide area contains sharp angled shaped crystal structures. EDX analysis of the images shows the presence of Cu and O uniformly distributed over the sample. The formation of these structures can be caused by bombardment of the surface by low energy plasma ions.[63]

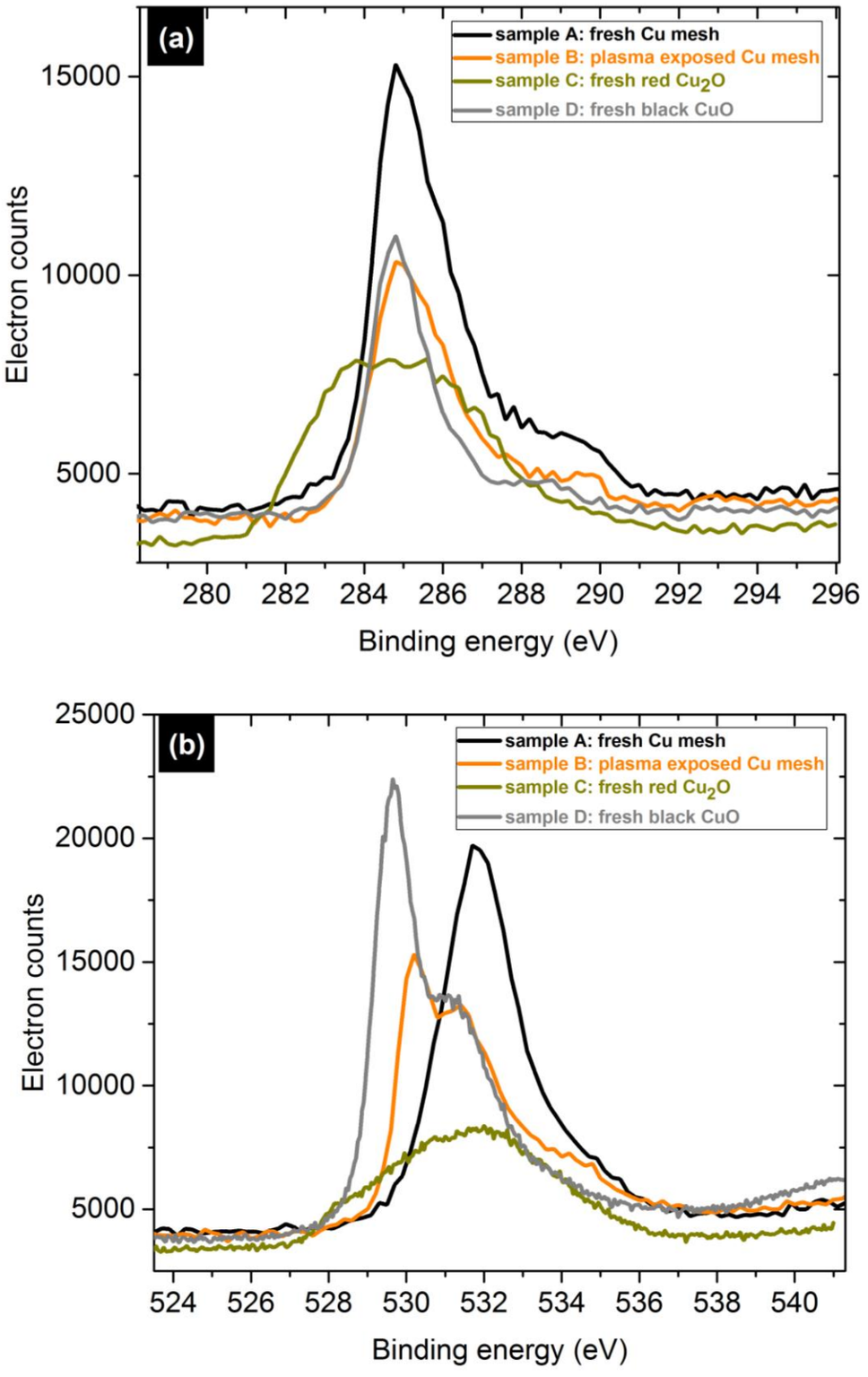

FIG. 4. (a) XPS spectra of C 1s of fresh and plasma exposed metal meshes, Data are shown for an as received Cu grid, the same grid exposed to CO_2 plasma. For reference. XPS spectra of Cu_2O and CuO powders are shown. (b) XPS spectra of O 1s for the same samples as shown in FIG. 4a.

Fig. 4 shows the XPS spectra of fresh and plasma exposed metal meshes. In the C1s spectra (Fig. 4a), the intensity of the peak is lower for the plasma exposed Cu mesh compared to the fresh one. This is due to the removal of carbonates on the metal grids by the CO_2 plasma. This decrease of the amount of carbon also shows that in the CO_2 dissociation no elemental carbon is formed, that is deposited on the metal grids in the reactor. We attribute the C signal observed for the Cu_2O and CuO powders to ambient carbon and residual carbonates in these powders, which were analysed as received. X-Ray Diffraction (XRD) analysis of the meshes, which we previously reported, confirmed the above analysis. [23]

Fig. 4b shows the O 1s region of the XPS spectrum. Plasma exposed metal mesh shows a shift toward lower binding energies (530 eV) with respect to the fresh sample, indicating that the presence of CuO with respect to Cu_2O has increased. The total amount of oxygen remains about the same. There is no oxygen uptake by the sample. The O s1 signal for the Cu_2O and CuO powders is shown for comparison.

The difference in mass of the plasma exposed metal mesh versus the fresh metal mesh is about 0.002 till 0.003 gram. This demonstrates that there is no uptake of O or C, nor removal of bulk metal.

The results presented in the previous section can be summarized by:

- Conversion into CO + O_2 does not occur in thermal catalysis at partial CO_2 pressures of 5000 Pa and up to 900 °C.
- In a RF-ICP reactor there is a dependence of the CO_2 conversion on reactor geometry and specific energy. Conversions of more than 50% can be observed in an empty catalyst holder (equipped with metal meshes and without catalyst pellets) inside the narrow tube plasma reactor at a specific energy of about 22 eV (Fig. 2).
- Inserting a metal grid or mesh increases the conversion rate significantly.
- Inserting a metal oxide supported catalyst does not increase the conversion rate.

The absence of thermal CO_2 conversion under 1000 °C is not surprising. The decomposition reaction is too endoergic to run at these temperatures. Vibrationally excited CO_2 will dissociate more easily at Ni surfaces.[44] Such excited molecules are absent in a thermal gas. Therefore, if any dissociation is observed in a plasma reactor, with or without catalyst, this is driven by a non-thermal plasma action.

The conversion scales with the amount of energy introduced into the plasma per molecule flowing through the plasma channel. We have observed previously that by diluting the CO_2 in Ar very high conversions (exceeding 90%) can be obtained.[28] The same conversion is seen when increasing the specific energy beyond 1000 eV.[20, 21] However, consequently the energy efficiency will be for both cases too low for any practical application. Insight into the plasma dynamics can be obtained from such experiments, for instance, that the electron temperature of the plasma should be kept low.

Inserting a metal mesh in our plasma reactors does increase the CO yield by at least a factor 1.2. There are several possible explanations for this. At first plasma parameters may be changed by the presence of the metallic object. However, visual inspection did not point to any change in the intensity of emitted light or the flow pattern. Optical Emission Spectroscopy data, shown in the Supplementary Material show the same spectrum as seen for a RF CO_2 arc without any catalyst.[64] So, we conclude that a surface reaction on the surface of the mesh is responsible. The first possibility we

considered is that the mesh acts as an oxygen scavenger. It is well known that recombination of CO + O + M => CO_2 is a significant loss channel for CO_2 conversion.[4] If the metal would absorb the reactive O-atoms, they are not available for recombination thereby increasing the conversion. This would lead to weight gain of the metal structure, but this is not observed. Also, in our XPS analysis concerning Fig. 4 the most important observations are a loss of C and O upon exposure of the metal. Our SEM images show a restructuring of the metal, similar to that of thermal oxidation of for instance Cu.[49, 55] We conclude that the surface of the metal mesh re-structures but it does not take up a large amount of oxygen. This is corroborated by the well documented fact that the diffusion of oxygen into a Cu lattice is limited.[55, 56]

Although XPS analysis shows that the surface is oxidized, this does not imply that the surface is oxidized during operation. During the transport of the metal from the reactor to the XPS machine, the sample is exposed to air for a long time and will be oxidized. The SEM picture in Fig. 3b shows that the surface has restructured, so the surface may have been (partially) metallic if oxygen is actively removed by the plasma and recombination via $O+O \rightarrow O_2$. This can be due to direct adsorption of free O-atoms at the surface of the metal or metal oxide. This will lead to a buildup of an oxygen atom coverage on the surface. Since in-diffusion of O-atoms is limited,[49, 55, 56] the adsorption of O-atoms will lead to recombinative desorption, resulting in the ejection of O_2 molecules. The reaction can be both a Langmuir-Hinshelwood type or an Eley-Rideal reaction.[65] Recently it was demonstrated that N-atoms created in a plasma are very efficient in removing O-atoms from a Ru surface by an Eley-Rideal reaction.[66] The O_2 molecules formed in turn can be dissociated in the plasma, but the rate is rather low and they will block recombination of CO + O leading to CO_2..[23] So, the presence of the metal structure acts as a catalyst for molecular recombination to O_2. This process keeps the O-coverage rather low and agrees with our XPS, XRD and SEM studies, demonstrating the growth of a surface oxide without loss of O-atoms into the bulk. We note again that the O-atoms are available in the gas phase, in contrast to a thermal catalytic reaction. In addition, the SEM images show erosion and restructuring of the surfaces by the plasma. It suggests that the solid metal catalyst is stable in a dynamic equilibrium with the plasma, while a supported metal-oxide catalyst is destroyed.

Another possibility for metal-induced CO yield increase is catalytic dissociation of CO_2 on metal surfaces (see Fig. 5). We have indicated that at least part of the surface will be metallic during operation. The SEM pictures show that the surface is very rough, and will contain many steps, facilitating CO_2 dissociation.[42, 43] It is known that CO_2 may dissociate upon impact of a vibrationally and translationally excited molecule on a metal. [44, 45] This is evident from an inspection of potential energy surfaces for CO_2-metal interactions. This will lead to O-atoms bound to the surface and weakly bound CO, that will desorb.[67] Although experimental and theoretical studies have focused on interactions at clean metal surfaces, this option is likely. Another option to enhance CO_2 dissociation is field induced dissociation, which was explored in a theoretical study.[46] The SEM images show that sharp structures develop on the metal meshes during operation. However, it is unlikely that these structures can directly lead to dissociation of CO_2, because the field strength required for field induced dissociation is very high. There is a strong similarity of the experimental results of all supported metal oxide catalysts in spite of their different physicochemical properties such as adsorption properties.[68] Therefore, it is likely that a supported Cu catalyst would not enhance CO_2 conversion either. In fact, Spencer and Gallimore have done experiments with Rh deposited on a

monolith.[20] Only a decrease in CO_2 conversion was observed, which demonstrates that only solid metallic catalysts have a clear catalytic action. If we would have taken a real thick film (micron size thickness) on a bead one can expect that behavior to be similar to the solid Cu meshes. Beads with such a coating were unavailable to us.

For ammonia production in plasma it was suggested that adding metal meshes leads to sputtering by the plasma of metal films on to the quartz walls of the reactor.[29] We consider this to be unlikely in the present case, because the onsets for CO formation in the QMS are very sharp, whereas an induction time can be expected if a catalytic film has to be built up in the process. This induction period can be seen in ref.[29].

Finally, looking at the plasma we see that not all plasma particles come in contact with the catalyst. The mean free path is small (less than 0.1 mm) so diffusion away from the flow direction will be limited. Designing structures with better contact between metal mesh recombination catalyst and flow may improve the conversion of CO_2 further.

Strong synergistic effects between plasma and catalysts have been found for DBD plasma.[4] We attribute the absence of such strong effects in the present work to the very different nature of the plasma for RF and DBD. The DBD consists of very inhomogeneous local high energy discharges. In the DBD the excitation of molecules is done by fast electrons, whereas in our case slow electrons drive the plasma. This leads to different active plasma species in case of the two plasmas. Also, as demonstrated in a recent paper, localized heating of the catalyst by the plasma could contribute to the synergy.[16] Finally, there is a big difference in pressure. DBD's work at atmospheric pressure, whereas the RF reactor works at a factor of 100 lower. Therefore, it is interesting to increase the pressure in the RF or quite similar MicroWave plasma to atmospheric. This has been done by Spencer and Gallimore, where a monolith was also used.[20] However, these authors have not seen any catalytic enhancement. These are absent in the RF plasma for supported catalysts.

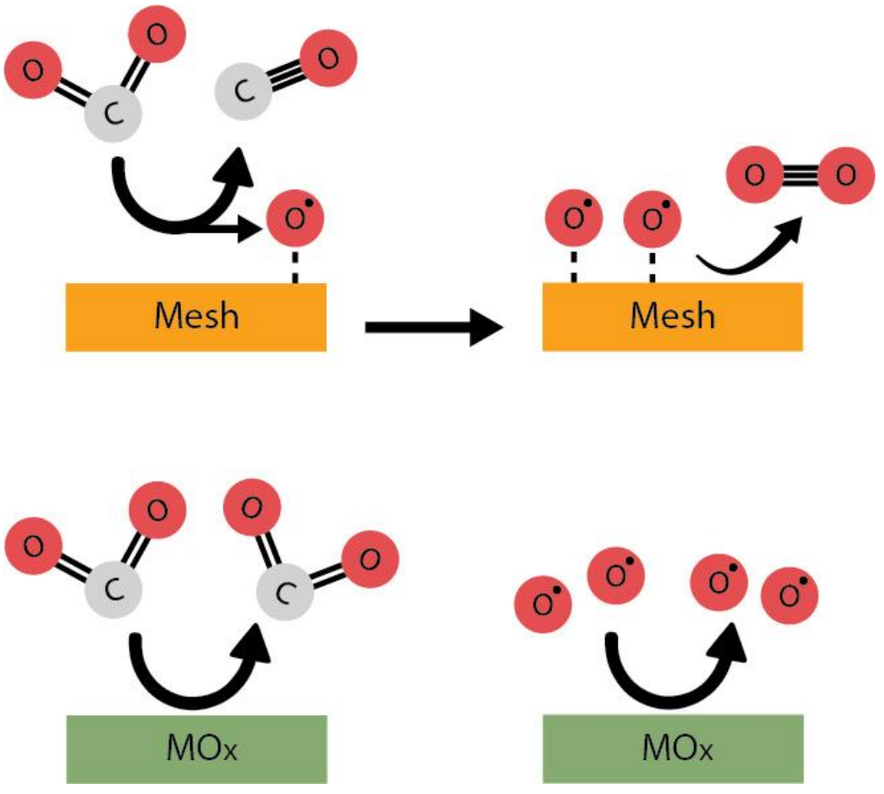

FIG. 5. Diagrams showing the proposed difference between the interaction of CO_2 (left panels) and O-atoms (right panels) with a metal mesh (upper panels) and a metal-oxide catalyst (lower panels). It shows that metal meshes break the CO-O bond and allow recombination of adsorbed atomic oxygen whereas for the metal-oxide catalyst this is less probable.

IV. CONCLUSION

We show that placing metallic structures such as meshes into the RF plasma reactor increases the CO_2 conversion by a factor of 1.2 to 1.8. The XPS analysis indicates that the metal does not absorb a significant amount of oxygen, but rather acts as a recombination catalyst towards molecular oxygen. In this way, the recombination of oxygen-atoms and CO to form CO_2 is suppressed in the plasma. In addition, the metallic surface of the Cu mesh will contain many steps and can break a CO-O bond. Both mechanisms are much less likely on an oxidic catalyst. The mechanisms are summarized in Fig. 5. Although the metal induced enhancement was demonstrated in our RF-ICP reactor. Metal induced enhancement will be active in other type of plasma reactors which provide primarily high energy efficiency, such as microwave plasma and thermal arc plasma. These results open a pathway to efficient plasma reactors for CO_2 conversion.

SUPPLEMENTARY MATERIAL

Journal of Applied Physics

AIP Publishing

Experimental setup configurations, catalyst preparation, catalyst testing by a thermal reactor, catalyst characterisation, optical emission spectroscopy of the plasma.

ACKNOWLEDGEMENTS

This work has the support of the National Natural Science Foundation of China (Grant No. 51561135013, 21603202, and 22072010). We thank the Netherlands Scientific Organisation (NWO) for the grant "Developing novel catalytic materials for converting CO2, methane and ethane to high-value chemicals in a hybrid plasma-catalytic reactor" (China.15.119).

DATA AVAILABILITY

Data available on request from the authors.

REFERENCES

1. R. J. Detz, J. N. H. Reek and B. C. C. van der Zwaan, Energy Environ. Sci. **11** (7), 1653-1669 (2018).
2. D. Hone, *Sky: Meeting the goals of the Paris agreement*. (Shell International B.V., https://www.shell.com/energy-and-innovation/the-energy-future/scenarios/shell-scenario-sky.html, 2018).
3. Y. Y. Birdja, E. Perez-Gallent, M. C. Figueiredo, A. J. Gottle, F. Calle-Vallejo and M. T. M. Koper, Nat. Energy **4** (9), 732-745 (2019).
4. R. Snoeckx and A. Bogaerts, Chem. Soc. Rev. **46** (19), 5805-5863 (2017).
5. M. Ronda-Lloret, G. Rothenberg and N. R. Shiju, ChemSusChem **12** (17), 3896-3914 (2019).
6. A. Bogaerts and E. C. Neyts, ACS Energy Lett. **3** (4), 1013-1027 (2018).
7. A. Bogaerts, T. Kozak, K. van Laer and R. Snoeckx, Faraday Discuss. **183**, 217-232 (2015).
8. X. M. Tao, M. G. Bai, X. A. Li, H. L. Long, S. Y. Shang, Y. X. Yin and X. Y. Dai, Prog. Energy Combust. Sci. **37** (2), 113-124 (2011).
9. W. C. Chung and M. B. Chang, Renew. Sust. Energ. Rev. **62**, 13-31 (2016).
10. L. Wang, Y. H. Yi, C. F. Wu, H. C. Guo and X. Tu, Angew. Chem.-Int. Edit. **56** (44), 13679-13683 (2017).
11. E. K. Gibson, C. E. Stere, B. Curran-McAteer, W. Jones, G. Cibin, D. Gianolio, A. Goguet, P. P. Wells, C. R. A. Catlow, P. Collier, P. Hinde and C. Hardacre, Angew. Chem.-Int. Edit. **56** (32), 9351-9355 (2017).
12. S. J. Xu, S. Chansai, C. Stere, B. Inceesungvorn, A. Goguet, K. Wangkawong, S. F. R. Taylor, N. Al-Janabi, C. Hardacre, P. A. Martin and X. L. Fan, Nat. Catal. **2** (2), 142-148 (2019).
13. L. Li, H. Zhang, X. D. Li, X. Z. Kong, R. Y. Xu, K. Tay and X. Tu, J. CO2 Util. **29**, 296-303 (2019).
14. P. Liu, X. S. Liu, J. Shen, Y. X. Yin, T. Yang, Q. Huang, D. Auerbach and A. W. Kleiyn, Plasma Sci. Technol. **21** (1), 4 (2019).
15. T. Y. Zhikai Li, Shaojun Yuan, Yongxiang Yin, Edwin J. Devid, Qiang Huang, Daniel Auerbach, Aart W. Kleyn, Jornal of Energy Chemistry **45**, 128-134 (2020).
16. D. Ray, D. Nepak, S. Janampelli, P. Goshal and C. Subrahmanyam, Energy Technol. **7** (4), 11 (2019).
17. A. H. Khoja, M. Tahir and N. A. S. Amin, Energy Conv. Manag. **183**, 529-560 (2019).

18. W. Bongers, H. Bouwmeester, B. Wolf, F. Peeters, S. Welzel, D. van den Bekerom, N. den Harder, A. Goede, M. Graswinckel, P. W. Groen, J. Kopecki, M. Leins, G. van Rooij, A. Schulz, M. Walker and R. van de Sanden, Plasma Process. Polym. **14** (6), 8 (2017).
19. G. J. van Rooij, D. C. M. van den Bekerom, N. den Harder, T. Minea, G. Berden, W. A. Bongers, R. Engeln, M. F. Graswinckel, E. Zoethout and M. de Sandena, Faraday Discuss. **183**, 233-248 (2015).
20. L. F. Spencer and A. D. Gallimore, Plasma Sources Science & Technology **22** (1), 9 (2013).
21. L. F. Spencer and A. D. Gallimore, Plasma Chemistry and Plasma Processing **31** (1), 79-89 (2011).
22. W. Jin, Q. Huang, H. Xu and A. W. Kleyn, in *Encyclopedia of Interfacial Chemistry: Surface Science and Electrochemistry*, edited by K. Kolasinsky and K. Wandelt (Elsevier Science Publishers, 2017).
23. E. Devid, M. Ronda-Lloret, D. Zhang, D. Wang, C.-h. Liang, Qiang Huang, G. Rothenberg, N. R. Shiju and A. Kleyn, Chin. J. Chem. Phys. **33** (2), 243-251 (2020).
24. E. J. Devid, D. Zhang, D. Wang, M. Ronda-Lloret, Q. Huang, G. Rothenberg, N. R. Shiju and A. Kleyn, Energy Technol., 1900886 (2020).
25. Q. Huang, D. Y. Zhang, D. P. Wang, K. Z. Liu and A. W. Kleyn, Journal of Physics D-Applied Physics **50** (29), 6 (2017).
26. Z. K. Li, T. Yang, S. J. Yuan, Y. X. Yin, E. J. Devid, Q. Huang, D. Auerbach and A. W. Kleyn, Journal of Energy Chemistry **45**, 128-134 (2020).
27. R. L. Yang, D. Y. Zhang, K. W. Zhu, H. L. Zhou, X. Q. Ye, A. W. Kleyn, Y. Hu and Q. Huang, Acta Phys.-Chim. Sin. **35** (3), 292-298 (2019).
28. D. Y. Zhang, Q. Huang, E. J. Devid, E. Schuler, N. R. Shiju, G. Rothenberg, G. van Rooij, R. L. Yang, K. Z. Liu and A. W. Kleyn, J. Phys. Chem. C **122** (34), 19338-19347 (2018).
29. J. Shah, W. Z. Wang, A. Bogaerts and M. L. Carreon, ACS Appl. Energ. Mater. **1** (9), 4824-4839 (2018).
30. H. Uyama, T. Nakamura, S. Tanaka and O. Matsumoto, Plasma Chemistry and Plasma Processing **13** (1), 117-131 (1993).
31. S. Tanaka, H. Uyama and O. Matsumoto, Plasma Chemistry and Plasma Processing **14** (4), 491-504 (1994).
32. J. Shah, T. Wu, J. Lucero, M. A. Carreon and M. L. Carreon, ACS Sustain. Chem. Eng. **7** (1), 377-383 (2019).
33. P. Peng, C. Schiappacasse, N. Zhou, M. Addy, Y. L. Cheng, Y. N. Zhang, K. Ding, Y. P. Wang, P. Chen and R. Ruan, ChemSusChem **12** (16), 3702-3712 (2019).
34. H. Patel, R. K. Sharma, V. Kyriakou, A. Pandiyan, S. Welzel, M. C. M. van de Sanden and M. N. Tsampas, ACS Energy Lett. **4** (9), 2091-2095 (2019).
35. M. L. Carreon, Journal of Physics D-Applied Physics **52** (48), 25 (2019).
36. M. Iwamoto, M. Akiyama, K. Aihara and T. Deguchi, ACS Catal. **7** (10), 6924-6929 (2017).
37. K. Aihara, M. Akiyama, T. Deguchi, M. Tanaka, R. Hagiwara and M. Iwamoto, Chem. Commun. **52** (93), 13560-13563 (2016).
38. U. Burghaus, Prog. Surf. Sci. **89** (2), 161-217 (2014).
39. U. Burghaus, Catal. Today **148** (3-4), 212-220 (2009).
40. I. A. Bonicke, W. Kirstein and F. Thieme, Surf. Sci. **307**, 177-181 (1994).
41. S. S. Fu and G. A. Somorjai, Surf. Sci. **262** (1-2), 68-76 (1992).
42. W. Taifan, J. F. Boily and J. Baltrusaitis, Surf. Sci. Rep. **71** (4), 595-671 (2016).
43. H. J. Freund and M. W. Roberts, Surf. Sci. Rep. **25** (8), 225-273 (1996).
44. B. Jiang and H. Guo, J. Chem. Phys. **144** (9), 5 (2016).
45. X. Y. Zhou, B. Kolb, X. Luo, H. Guo and B. Jiang, J. Phys. Chem. C **121** (10), 5594-5602 (2017).
46. A. Jafarzadeh, K. M. Bal, A. Bogaerts and E. C. Neyts, J. Phys. Chem. C **124** (12), 6747-6755 (2020).
47. X. Duan, O. Warschkow, A. Soon, B. Delley and C. Stampfl, Phys. Rev. B **81** (7), 15 (2010).
48. A. Soon, M. Todorova, B. Delley and C. Stampfl, Phys. Rev. B **73** (16), 12 (2006).

49. C. Gattinoni and A. Michaelides, Surf. Sci. Rep. **70** (3), 424-447 (2015).
50. M. E. Turano, R. G. Farber, E. C. N. Oskorep, R. A. Rosenberg and D. R. Killelea, J. Phys. Chem. C **124** (2), 1382-1389 (2020).
51. R. G. Farber, M. E. Turano, E. C. N. Oskorep, N. T. Wands, L. B. F. Juurlink and D. R. Killelea, J. Phys.-Condes. Matter **29** (16), 5 (2017).
52. J. Derouin, R. G. Farber and D. R. Killelea, J. Phys. Chem. C **119** (26), 14748-14755 (2015).
53. J. Derouin, R. G. Farber, M. E. Turano, E. V. Iski and D. R. Killelea, ACS Catal. **6** (7), 4640-4646 (2016).
54. J. Derouin, R. G. Farber, S. L. Heslop and D. R. Killelea, Surf. Sci. **641**, L1-L4 (2015).
55. J. C. Yang, B. Kolasa, J. M. Gibson and M. Yeadon, Appl. Phys. Lett. **73** (19), 2841-2843 (1998).
56. C. Boas, J. M. Sturm and F. Bijkerk, J. Appl. Phys. **126** (15) (2019).
57. Y. X. Yao, P. Shushkov, T. F. Miller and K. P. Giapis, Nature Communications **10**, 1 (2019).
58. N. Madaan, R. Haufe, N. R. Shiju and G. Rothenberg, Topics in Catalysis **57** (17-20), 1400-1406 (2014).
59. Q. Z. Zhang and A. Bogaerts, Plasma Sources Science & Technology **27** (3), 10 (2018).
60. Q. Q. Jiang, Z. P. Chen, J. H. Tong, M. Yang, Z. X. Jiang and C. Li, ACS Catal. **6** (2), 1172-1180 (2016).
61. J. S. Zhang, V. Haribal and F. X. Li, Sci. Adv. **3** (8), 8 (2017).
62. M. Tou, R. Michalsky and A. Steinfeld, Joule **1** (1), 146-154 (2017).
63. E. Taglauer and W. Heiland, J. Nucl. Mat. **93-4** (OCT), 823-829 (1980).
64. C. Rond, A. Bultel, P. Boubert and B. G. Cheron, Chem. Phys. **354** (1-3), 16-26 (2008).
65. A. W. Kleyn, Chem. Soc. Rev. **32** (2), 87-95 (2003).
66. T. Zaharia, A. W. Kleyn and M. A. Gleeson, Phys. Rev. Lett. **113** (5) (2014).
67. S. Vollmer, G. Witte and C. Woll, Catal. Lett. **77** (1-3), 97-101 (2001).
68. E. J. Ras, M. J. Louwerse, M. C. Mittelmeijer-Hazeleger and G. Rothenberg, PCCP **15** (12), 4436-4443 (2013).

AIP Publishing

Journal of Applied Physics

ACCEPTED MANUSCRIPT

This is the author's peer reviewed, accepted manuscript. However, the online version of record will be different from this version once it has been copyedited and typeset.
PLEASE CITE THIS ARTICLE AS DOI: 10.1063/5.0033212

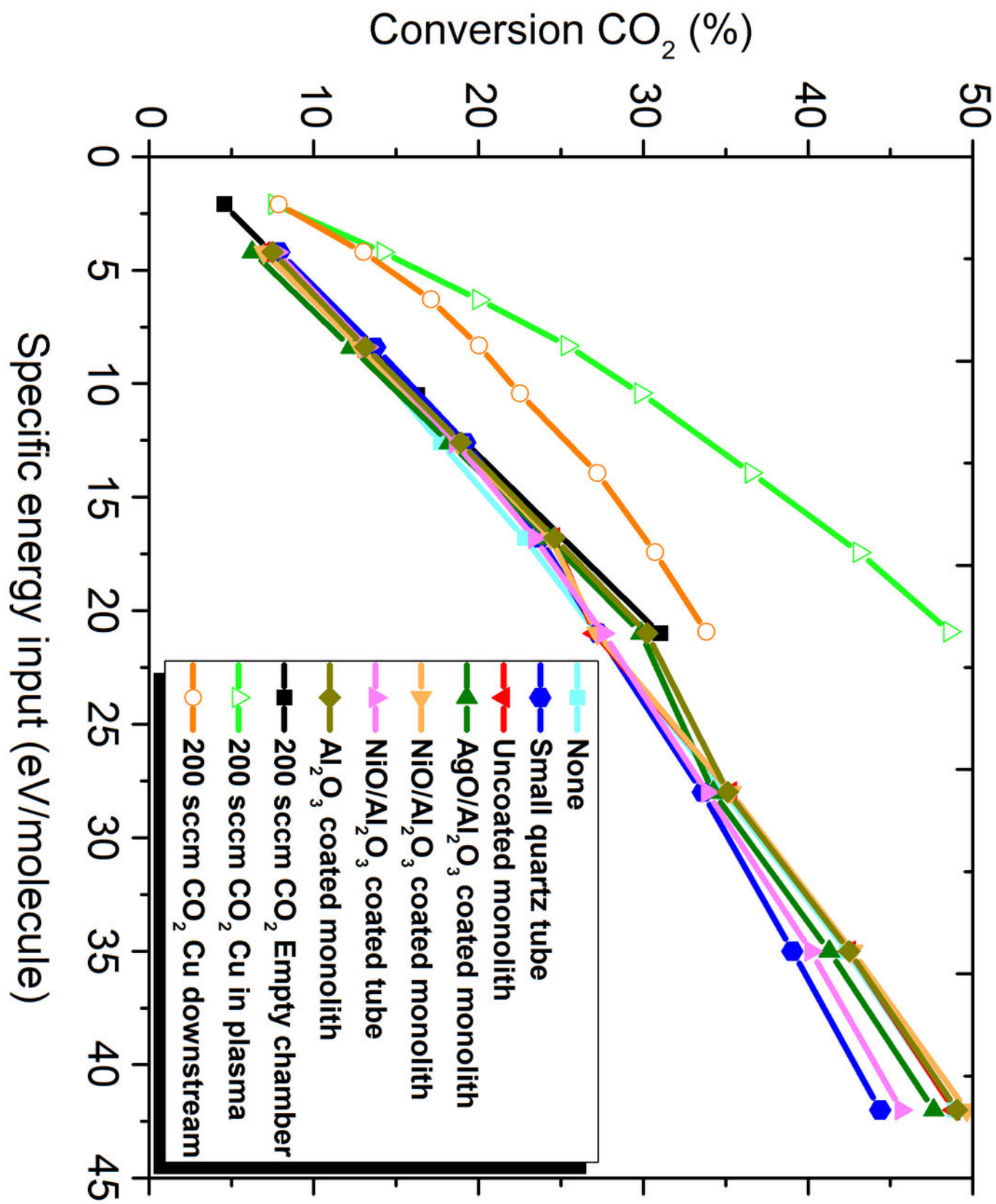

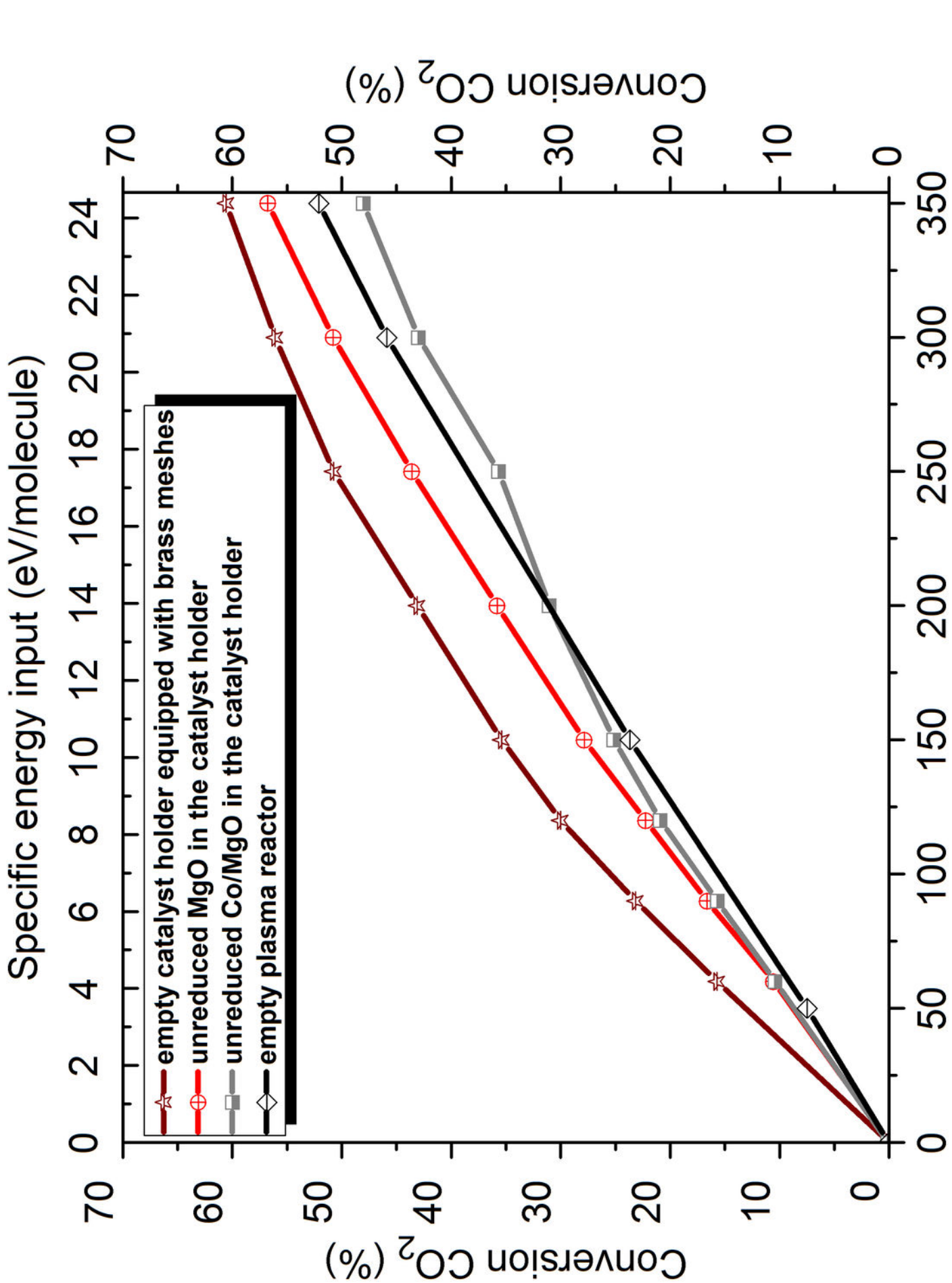

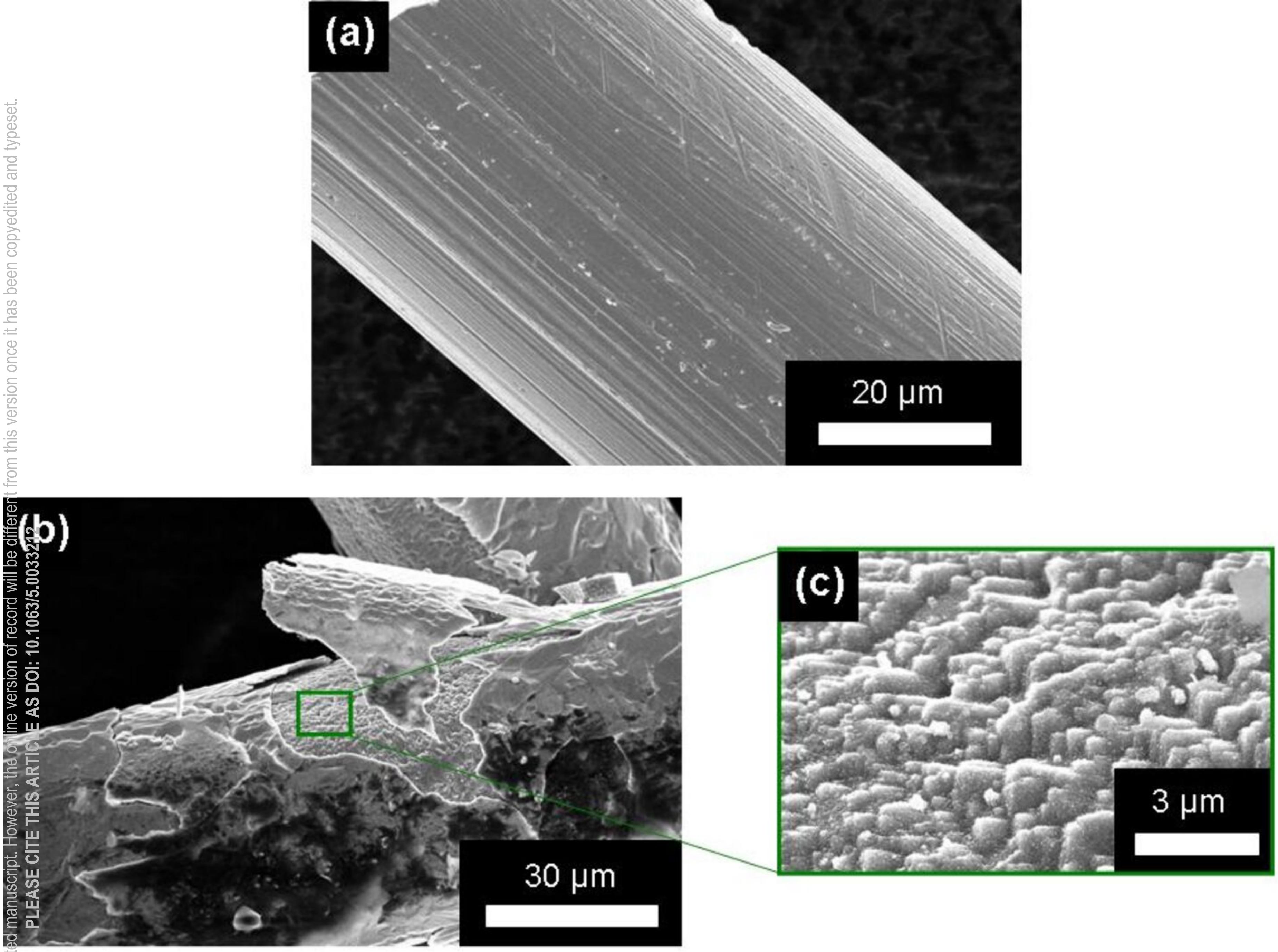

Journal of Applied Physics

PLEASE CITE THIS ARTICLE AS DOI: 10.1063/5.0033212

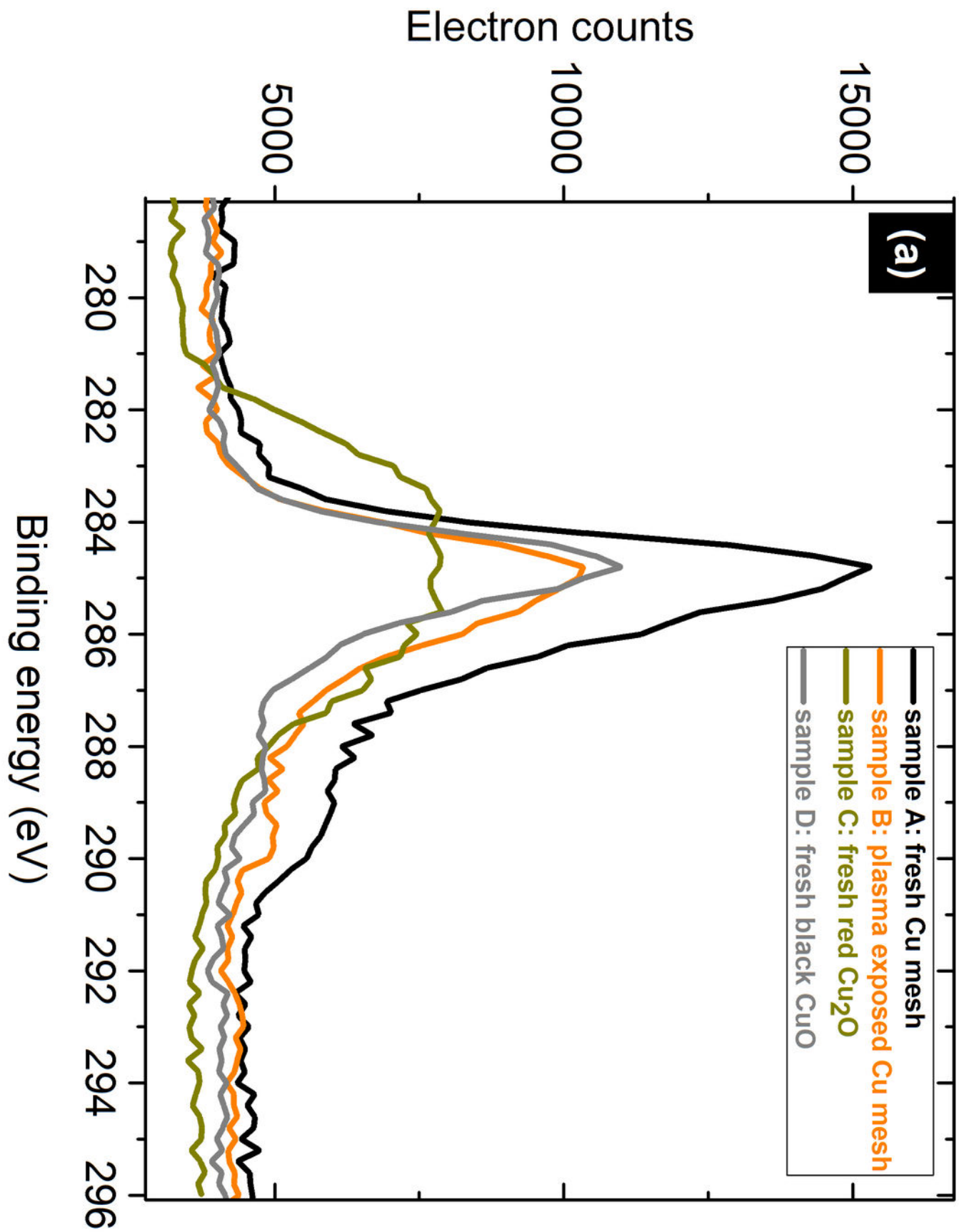

AIP Publishing

Journal of Applied Physics

ACCEPTED MANUSCRIPT

This is the author's peer reviewed, accepted manuscript. However, the online version of record will be different from this version once it has been copyedited and typeset.
PLEASE CITE THIS ARTICLE AS DOI: 10.1063/5.0033212

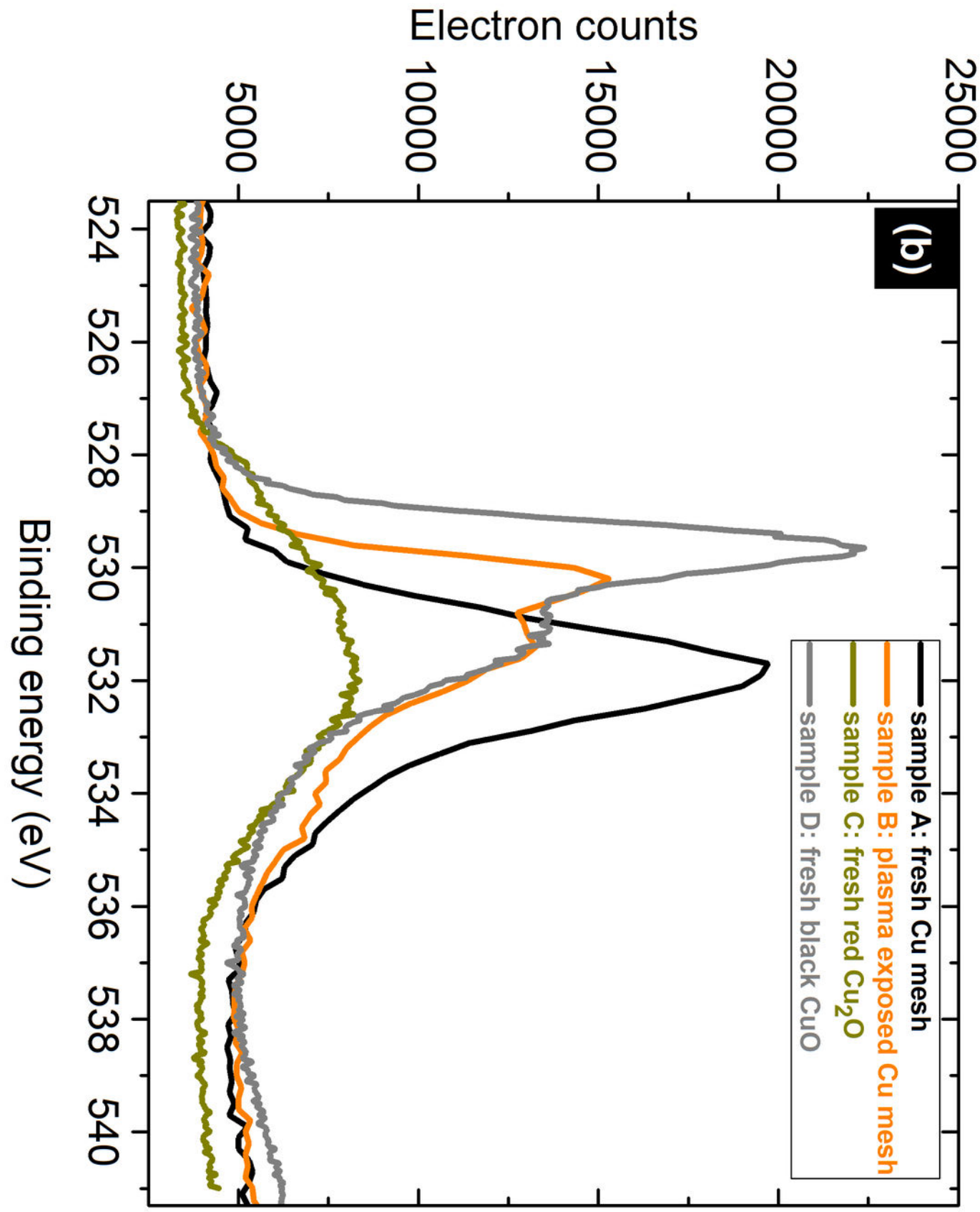

AIP Publishing

Journal of Applied Physics

ACCEPTED MANUSCRIPT

PLEASE CITE THIS ARTICLE AS DOI: 10.1063/5.0033212